

---

# Big-Data Clustering: K-Means or K-Indicators?

---

Feiyu Chen\*  
fchen@cqu.edu.cn

Yuchen Yang†  
yuchen.yang@rice.edu

Liwei Xu‡  
xul@uestc.edu.cn

Taiping Zhang§  
tpzhang@cqu.edu.cn

Yin Zhang†¶  
yinzhang@cuhk.edu.cn

## Abstract

The K-means algorithm is arguably the most popular data clustering method, commonly applied to processed datasets in some "feature spaces", as is in spectral clustering. Highly sensitive to initializations, however, K-means encounters a scalability bottleneck with respect to the number of clusters  $K$  as this number grows in big data applications. In this work, we promote a closely related model called K-indicators model and construct an efficient, semi-convex-relaxation algorithm that requires no randomized initializations. We present extensive empirical results to show advantages of the new algorithm when  $K$  is large. In particular, using the new algorithm to start the K-means algorithm, without any replication, can significantly outperform the standard K-means with a large number of currently state-of-the-art random replications.

## 1 Introduction

Clustering analysis is a fundamental unsupervised machine learning strategy with broad-ranging applications, aiming to group unlabelled data objects into clusters according to a certain similarity measure so that objects within each cluster are more similar to each other than otherwise.

Many clustering algorithms have been investigated in the past decades [7, 24, 26]. In practice, clustering-friendly datasets rarely occur in nature, which makes it necessary to employ a two-step strategy. First, the raw data was kernelized [25, 9] or otherwise preprocessed with dimension reduction methods, such as principal component analysis [10], non-negative matrix factorization [31, 11], spectral embeddings [28, 20, 33], deep auto-encoders [23, 16, 27] or generative adversarial networks [6]. Second, a clustering algorithm is applied to the latent embedding. Many clustering methods exist for the doing the second step, including K-means [19, 18], hierarchical clustering [29], affinity propagation [12] and BIRCH [34], etc, among which the classic K-means is arguably the method of choice in general situations.

Unfortunately, even with well-processed data the K-means algorithm (also called Lloyd algorithm) still encounters a scalability bottleneck. It is demonstrated in Figure 1 that the solution quality of the K-means algorithm deteriorates as the number of clusters increases, while a newly proposed algorithm, called KindAP to be introduced soon, correctly recover the ground truth solutions in all tested cases. This set of experiments is performed on synthetic datasets with separable clusters (see more details in the caption of Figure 1). Later we will show that similar phenomena occur in real image datasets as well.

---

\*School of Big Data and Software Engineering, Chongqing University, Chongqing, China

†Department of Computational and Applied Mathematics, Rice University, Houston, Texas, U.S.A.

‡School of Mathematical Sciences, University of Electronic Science and Technology of China, Chengdu, Sichuan, China

§College of Computer Science, Chongqing University, Chongqing, China

¶Institute for Data and Decision Analytics, The Chinese University of Hong Kong-Shenzhen, China

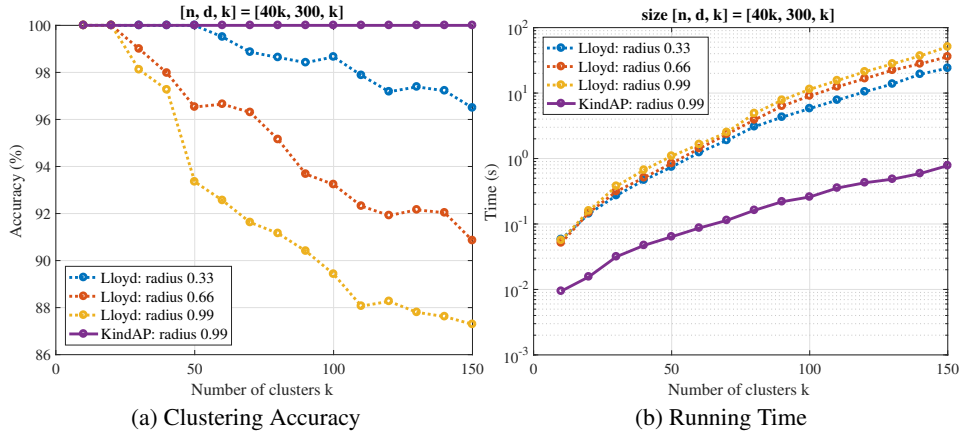


Figure 1: Synthetic data clouds: we select  $k$  center locations in  $\mathbb{R}^{300}$ , where  $k$  varies from 10 to 150, such that the distance between each pair of centers is exactly 2. Then 40 data points are randomly placed on a sphere of radius  $\rho = \{0.33, 0.66, 0.99\}$  around each center to form a cluster. The processed datasets consist of rows of the  $n \times k$  matrix formed by the  $k$  leading singular vectors of the  $n \times 300$  data matrix for  $n = 40k$ . The Lloyd algorithm (with 10 random replications) and the proposed KindAP algorithm are applied to the processed data matrices. Clustering accuracy and running time are recorded.

The root cause of the scalability bottleneck is that greedy algorithms like K-means are highly sensitive to initializations and rely on multiple random replications to achieve good results. As  $K$  increases, the number of random replications needed for good results appears to rise out of control. To overcome this difficulty, some convex optimization models have been developed. Recent works include semi-definite programming (SDP) [22, 2] and linear programming (LP) relaxations [2] of K-means, and convex fusion methods [17, 14, 8]. However, the per-iteration complexity of these convex models has been elevated to being quadratic in the number of total samples instead of being linear as in K-means.

In the framework of spectral clustering, an algorithm called spectral rotation (SR) was proposed as an alternative to K-means algorithm [32, 15] for doing clustering in embedded spaces. It was argued that the spectral rotation model would be less sensitive to initializations than K-means. Nevertheless, our experiments (see Section 6) indicate that, at least in some cases, the spectral rotation algorithm could be as sensitive as the K-means.

The main contributions of this paper are summarized as the following:

- A general clustering framework is proposed that directly solves for  $K$  indicators by subspace matching. Under suitable conditions, K-means model and the model that we promote are two special cases of the general clustering framework.
- A semi-convex-relaxation scheme, called KindAP, is constructed to efficiently solve the particular K-indicators model. KindAP, which is essentially deterministic, can find high-quality solutions at a per-iteration complexity linear in the number of data points.
- KindAP solutions can be used to warm-start the K-means algorithm without any replication, resulting in better results (measured by the K-means objective) than running K-means with a huge number of K-means++ random replications, when  $K$  is relatively large.
- Extensive numerical results show a superior scalability of the proposed approach over both K-means and spectral rotation models, especially when the number of clusters becomes large.

## 2 Preliminary

This section provides important definitions and concepts for our study. It also revisits the classical K-means model from an unusual angle that will motivate our new K-indicators model.

### 2.1 A set of indicator matrices

Consider the problem of clustering a dataset of  $n$  objects into  $k$  clusters. A matrix  $H \in \mathbb{R}^{n \times k}$  is called an indicator matrix if:

$$H_{ij} = \begin{cases} c_{ij} > 0, & \text{object } i \in \text{cluster } j \\ 0, & \text{otherwise} \end{cases} \quad (1)$$

where a positive element  $H_{ij} = c_{ij}$  indicates that object  $i$  belongs to cluster  $j$ . This set of indicator matrices is the most general, containing various subsets corresponding to different definitions of indicator matrices in the literature. For example,  $H$  is called a *binary indicator matrix* if  $c_{ij} \equiv 1$  [32], and a *normalized indicator matrix* if  $c_{ij} \equiv 1/\sqrt{n_j}$ , where  $n_j$  denotes the number of objects in cluster  $j$  [4].

For convenience, by default we define the set of indicator matrices as:

**Definition 2.1.** (*The set of indicator matrices*)

$$\mathcal{H} = \{H \in \mathbb{R}^{n \times k} : H^T H = I, H \geq 0, \|e_i^T H\|_0 = 1\} \quad (2)$$

Clearly,  $\mathcal{H}$  is a discrete set since each row of  $H$  can have only one positive element. To emphasize the pre-determined number  $k$ , we will refer the  $k$  columns of  $H$  collectively as K-indicators. These two terms, indicator matrix and K-indicators, will be used exchangeably.

### 2.2 K-means model viewed as subspace-matching

Although the classic K-means model is commonly written in terms of  $k$  centroids, it can also be written in terms of indicator matrices, or K-indicators. Let  $\hat{U} \in \mathbb{R}^{n \times d}$  be a given data matrix where each data vector in  $\mathbb{R}^d$  corresponds to a row. It is well known that the classical K-means model can also be rewritten as [4]:

$$\min_H \|\hat{U} - HH^T \hat{U}\|_F^2 \quad \text{s.t. } H \in \mathcal{H}_0 := \mathcal{H} \cap \{H \mid HH^T \mathbf{1}_n = \mathbf{1}_n\} \quad (3)$$

where the constraint  $HH^T \mathbf{1}_n = \mathbf{1}_n$ , together with other constraints in  $\mathcal{H}$ , forces non-zero elements in each column of  $H$  to have the same value (i.e.,  $1/\sqrt{n_j}$ ). In other words,  $\mathcal{H}_0$ , the subset of  $\mathcal{H}$ , contains all normalized indicator matrices.

When the data matrix  $\hat{U} \in \mathbb{R}^{n \times d}$  ( $d \geq k$ ) is orthonormal, i.e.  $\hat{U}^T \hat{U} = I$ , then after some simple calculations the K-means model (3) can be reduced to the following three equivalent optimization problems:

$$\min_{H \in \mathcal{H}_0} \|\hat{U} \hat{U}^T - HH^T\|_F^2 \Leftrightarrow \max_{H \in \mathcal{H}_0} \|\hat{U}^T H\|_F^2 \Leftrightarrow \max_{H \in \mathcal{H}_0} \sum_{j=1}^k \sigma_j^2(\hat{U}^T H) \quad (4)$$

where  $\sigma_j(\cdot)$  denotes the  $j$ -th singular values of a matrix. We note that taking square root of these objective functions does not change the equivalence.

These relationships provide a subspace-matching perspective for the K-means model. To see this, we note that the distance of two subspaces can be measured by a distance between their unique orthogonal projections. For the first model in (4), the two orthogonal projections involved are  $\hat{U} \hat{U}^T$  and  $HH^T$ , respectively. On the other hand, minimizing a subspace distance under some norms is equivalent to maximizing vector norms of the cosines of principle angles between the two subspaces [3]. In (4), these cosines of principle angles are the singular values of  $\hat{U}^T H$  where both  $\hat{U}$  and  $H$  are orthonormal bases.

### 3 K-indicators Model

The subspace-matching perspective of the K-means model can be extended to a more general framework that solves for an indicator matrix. We will call it K-indicators framework:

$$\min_H \text{dist}(\mathcal{R}(\hat{U}), \mathcal{R}(H)), \text{ s.t. } H \in \mathcal{H} \quad (5)$$

where  $\mathcal{R}(\hat{U})$  refers to the range space of  $\hat{U}$  (similarly for  $\mathcal{R}(H)$ ), and "dist" is a subspace distance, which can also be replaced by distance squared, for example. Clearly, in the K-means model (3) the squared distance function  $\|\hat{U}\hat{U}^T - HH^T\|_F^2$  is quartic in  $H$  and non-convex. Can we have a simpler distance function in  $H$ ?

**Theorem 3.1.** *If  $\hat{U} \in \mathbb{R}^{n \times k}$  such that  $\hat{U}^T \hat{U} = I$ , and  $H \in \mathbb{R}^{n \times k}$  such that  $H^T H = I$ , then*

$$\text{dist}(\mathcal{R}(\hat{U}), \mathcal{R}(H)) := \min_{R^T R = I} \{\|\hat{U}R - H\|_F : R \in \mathbb{R}^{k \times k}\} \quad (6)$$

defines a distance between  $\mathcal{R}(\hat{U})$  and  $\mathcal{R}(H)$ ,

$$\min_{H \in \mathcal{H}} \text{dist}^2(\mathcal{R}(\hat{U}), \mathcal{R}(H)) \Leftrightarrow \max_{H \in \mathcal{H}} \|\hat{U}^T H\|_* \Leftrightarrow \max_{H \in \mathcal{H}} \sum_{j=1}^k \sigma_j(\hat{U}^T H). \quad (7)$$

Moreover,

$$\frac{\sqrt{2}}{2} \|\hat{U}\hat{U}^T - HH^T\|_F \leq \min_{R^T R = I} \|\hat{U}R - H\|_F \leq \|\hat{U}\hat{U}^T - HH^T\|_F \quad (8)$$

The proof of this theorem is provided in the supplementary material.

Now, we propose the following model based on the distance function (6):

$$\min_{U, H} \|U - H\|_F^2, \text{ s.t. } H \in \mathcal{H}, U \in \mathcal{U} = \{\hat{U}R \mid R \in \mathbb{R}^{k \times k}, R^T R = I\} \quad (9)$$

For convenience, we will refer to this model as the K-indicators model. Other models of course can be constructed using different distance functions in (5).

Theorem 3.1 reveals the relations between the K-means model (3) and the K-indicators model (9). Both minimize a distance between the "data space"  $\mathcal{R}(\hat{U})$  and "indicator space"  $\mathcal{R}(H)$ , or both maximize a norm of the matrix  $\hat{U}^T H$ . In either case,  $H$  varies in a set of indicator matrices. In terms of the singular values of  $\hat{U}^T H$ , the difference between K-means model (3) and K-indicators model (9) lies in using  $l_2$ -norm or  $l_1$ -norm. It is important to note that the two models are distinct, thus may give distinct solutions at optimality, but quite close as is indicated by inequalities in (8).

### 4 KindAP Algorithm

We seek to design an algorithm for the K-indicators model (9) that has the potential to overcome the aforementioned scalability bottleneck. We have seen that the objective in (3) for K-means is by itself non-convex as a function of  $H$ . In contrast, the objective in (9) for K-indicators is convex in  $H$ , representing a squared distance between two sets,  $\mathcal{U}$  and  $\mathcal{H}$ , both of which are non-convex sets. Among the two,  $\mathcal{H}$  is extremely non-convex with a combinatorial structure. On the other hand,  $\mathcal{U}$  is less difficult to handle. For one thing, the projection onto  $\mathcal{U}$  is unique in generic cases.

Our idea is to break the difficult problem of solving model (9) into solving a sequence of sub-problems that satisfy two criteria: (i) each one is easier to solve, and (ii) iteration complexity is kept at linear in  $n$ . In a balance of the two criteria, we propose a semi-convex-relaxation scheme: introducing a convex relaxation to  $\mathcal{H}$  but keeping  $\mathcal{U}$  unchanged. This leads to an intermediate problem:

$$\min_{U, N} \|U - N\|_F^2, \text{ s.t. } U \in \mathcal{U}, N \in \mathcal{N} \quad (10)$$

where  $\mathcal{N} = \{N \in \mathbb{R}^{n \times k} \mid 0 \leq N \leq 1\}$  is a closed convex set whose boundary contains  $\mathcal{H}$ .

The projection onto  $\mathcal{N}$  is trivial, while the projection onto  $\mathcal{U}$  is the so-called Procrustes problem. The closed forms of the two projections are collected into Proposition 4.1 below.

**Proposition 4.1.** *The projection of matrix  $U \in \mathbb{R}^{n \times k}$  onto the set  $\mathcal{N}$  is given by*

$$\mathcal{P}_{\mathcal{N}}(U) = \max(\mathbf{0}, U), \quad (11)$$

*and the projection of matrix  $N \in \mathbb{R}^{n \times k}$  onto the set  $\mathcal{U}$  is given by*

$$\mathcal{P}_{\mathcal{U}}(N) = U(PQ^T) \quad (12)$$

*where  $U \in \mathcal{U}$  is an arbitrary orthonormal basis of  $\mathcal{R}(\hat{U})$ , and  $U^T N = P\Sigma Q^T$  is a singular value decomposition of the matrix  $U^T N \in \mathbb{R}^{k \times k}$ .*

An alternating projection algorithm [30] appears a natural choice for attacking the semi-relaxation model (10), for which the computational complexity of the two projections, onto  $\mathcal{U}$  and  $\mathcal{N}$ , remains linear with respect to  $n$ .

On top of the above semi-convex-relaxation scheme, we construct a double-layered alternating projection framework for approximately solving the K-indicators model (9). See Fig.2 for a schematic description. In our algorithm, each outer iteration consists of a loop going from  $\mathcal{U}$  to  $\mathcal{H}$  and then coming back. The route from  $\mathcal{U}$  to  $\mathcal{H}$  takes a detour to  $\mathcal{N}$  by solving the semi-convex model (10) via alternating projections, which are called inner iterations. The inner or the outer iteration is stopped once a prescribed amount of improvement in the relevant objective value is no longer observed. We name this algorithm KindAP (K-indicators by Alternating Projections).

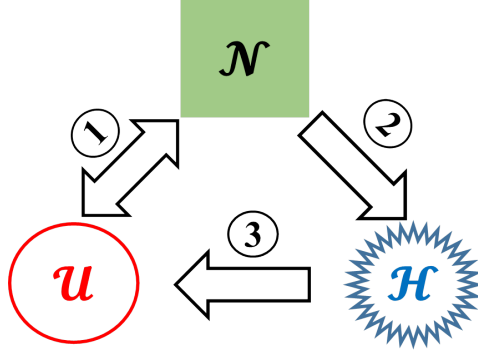


Figure 2: Big picture of KindAP: Step 1 is inner alternating projection iterations for solving (10). Step 2 is a rounding procedure to convert the solution of Step 1 in  $\mathcal{N}$  into an indicator matrix by keeping only one nonzero, the largest, for each row. Step 3 projects the indicator matrix back to  $\mathcal{U}$  to restart a new outer iteration.

## 5 Related Works

This section clarifies the relationship between our study and other relevant works. In the framework of spectral clustering, an approach called Program of Optimal Discretization (POD) is proposed to compute a binary indicator matrix  $B$  and a rotation matrix  $R$  from an input matrix  $\hat{U} \in \mathbb{R}^{n \times k}$  consisting of  $k$  leading eigenvectors of a normalized Laplacian matrix [32]. The model is

$$\min_{B,R} \|\hat{U}R - B\|_F^2 \quad \text{s.t. } B \in \mathcal{B}, R^T R = I \quad (13)$$

where  $\mathcal{B} = \{B \in \{0, 1\}^{n \times k} : B\mathbf{1}_k = \mathbf{1}_n\}$  is the set of binary indicator matrices. The model aims to find a rotation matrix  $R$  to best match  $\hat{U}R$  by a binary indicator matrix  $B$ . The POD model is also called spectral rotation (SR) in [15]. An ‘‘alternating projection’’ type algorithm for solving the SR model was proposed. For a fixed  $R$ , the binary indicator matrix  $B$  is computed by

$$B_{ij} = \begin{cases} 1, & \text{if } j = \arg \min_{j'} \|u_i - r_{j'}\|_2 \\ 0, & \text{otherwise} \end{cases} \quad (14)$$

where  $u_i$  is the  $i$ -th row of  $U$  and  $r_{j'}$  is the  $j'$ -th row of  $R^T$ . For a fixed  $B$ , the rotation matrix  $R$  is given by

$$R = QP^T \quad (15)$$

where  $P$  and  $Q$  are formed by the left and right singular vectors of  $\hat{U}^T B$ , respectively.

There are two main differences between the SR and the K-indicators clustering approaches. The first one is about the two models which do look rather similar in appearance. Mathematically, the K-indicators framework is based on subspace matching, that is, minimizing a distance or a measure of principle angles between two subspaces. On the other hand, the motivation of the SR model was to add the orthonormal restriction to the matrix  $R^T$  whose rows represent  $k$  centers (note that in K-means model these centers are unrestricted). Indeed, since the columns of  $B$  do not form an orthonormal basis, the SR objective does not mathematically define a subspace distance and the singular values of  $\hat{U}^T B$  are not cosines of principle angles.

The second difference is about the algorithms used. For the K-indicators model, we propose a double-layered alternating projection framework based on a semi-convex-relaxation scheme, which is essentially a deterministic algorithm. In the SR algorithm, formula (14) is still greedy in nature that makes the algorithm vulnerable to the same scalability bottleneck encountered by K-means, as we will see in Section 6.

Moreover, an extra benefit of using KindAP is that the intermediate variable  $N$  in (10) produces posteriori information to evaluate the clustering quality in the absence of ground truth knowledge. Please see more details in supplementary materials.

## 6 Numerical Experiments

KindAP performs well on synthetic datasets in terms of both quality and efficiency, as is seen in Figure 1. However, we need to validate it on “real” datasets commonly used in the literature. This section contains results from extensive numerical experiments on many real datasets.

All the algorithms used in this section are implemented and run in Matlab R2018a. To be specific, the Lloyd algorithm in use is the Matlab’s `kmeans` function with GPU support and the K-means++ [1] initialization strategy. In our notation, “KM  $m$ ” denotes running the Lloyd algorithm with  $m$  random replications in its default setting. In this section, KM 1, KM 10, KM 30, and KM 10000 will be used. KindAP is the proposed algorithm, and KindAP+L is a combination of KindAP and Lloyd in which the former is first run and the resulting centers are used to initialize the latter without further replication. We implement the SR algorithm based on [15]. Due to SR’s sensitivity to initialization, we also run it with multiple random replications and output the best solution with the lowest SR objective value. Similarly, we use the term “SR  $m$ ” to denote running the SR algorithm with  $m$  random replications. Our code is available at <https://github.com/yangyuchen0340/Kind>. This package also contains a Python implementation, which is consistent with the well-known `sklearn` package containing tools for data mining and data analysis. We remark that the package supports SR and KindAP in the same function, and allows a flexibility in selecting different types of indicator matrices for KindAP.

### 6.1 Deterministic behavior of KindAP

First, we show that KindAP algorithm is robust and essentially deterministic, as is demonstrated on two datasets YaleB and COIL100, both preprocessed by a technique called Deep Subspace Clustering [16]. Six algorithms are tested, each with 200 random runs. The maximum, minimum, and the standard deviation of clustering accuracy are plotted in Figure 3.

As is expected, Figure 3 shows that random replications can reduce the deviation of accuracy for both K-means and SR. Most importantly, we observe that KindAP and KindAP+L are essentially deterministic on these two examples, achieving the identical clustering result in 200 independent random runs. Interestingly, on both these two examples the K-indicators model happens to give much better clustering accuracy than the K-means model does. Moreover, when solving the K-means model for these two examples, KindAP+L produces higher accuracy than both KM 1 and KM 10 with 200 random replications (2000 replications in total for the latter).

### 6.2 Results on 35 real datasets

In this set of experiments, we compare the clustering accuracy and the K-means objective values between KindAP+L and KM 10000 on 35 real datasets. They include many UCI datasets, image and

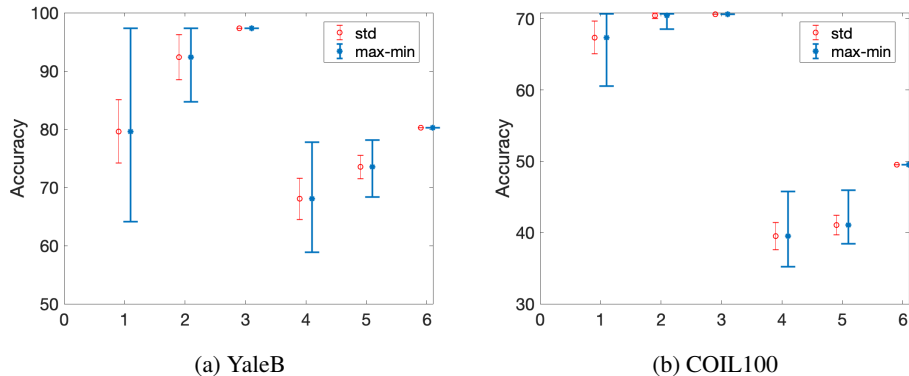


Figure 3: The distribution of clustering accuracy by 6 different algorithms with 200 random runs. Algorithms from left to right: SR 1, SR 10, KindAP, KM 1, KM 10, KindAP+L

NLP datasets, with  $k$  ranging from  $k = 2$  to  $k = 120$ . Although the underlying structures of these datasets vary from set to set, for practical reasons we preprocess all the 35 raw datasets uniformly by the normalized cut [28, 20] of their  $k$ -nearest-neighbor similarity graphs [5]. As a result, the clustering quality is not uniformly high.

Datasets	$k$	Clustering Accuracy		Objective Value	
		KindAP+L	KM 10000	KindAP+L	KM 10000
YaleB	38	<b>36.54%</b>	36.50%	6.0864e+00	<b>6.0858e+00</b>
ORL	40	<b>67.00%</b>	66.50%	6.3029e+00	<b>6.0932e+00</b>
Reuters	65	<b>39.36%</b>	39.26%	<b>9.4345e+00</b>	1.0090e+01
PIE	68	16.17%	<b>16.90%</b>	<b>1.0711e+01</b>	1.2179e+01
FERET	72	<b>66.20%</b>	66.20%	<b>1.3391e+01</b>	1.3398e+01
AR	120	<b>60.48%</b>	58.33%	<b>1.5452e+01</b>	1.7324e+01

Table 1: Comparison of Clustering performance on 6 datasets with  $k \geq 38$ . Results with the highest clustering accuracy or the lowest objective value are highlighted in bold.

It turns out that on the 29 datasets with  $k \leq 20$ , KindAP+L and KM 10000 have obtained the identical clustering accuracies, presumably corresponding to the global optima for the given datasets (see more details in the supplementary material).

The results for the remaining six datasets with  $k \geq 38$  are reported in Table 1. We observe that on the two datasets with  $k \leq 40$ , KM 10000 reached smaller K-means objective values, but on the four datasets with  $k \geq 65$  KindAP obtained better objective values, in fact significantly better in 3 out of the 4 cases. The fact that a single KindAP run provides better initializations than 10000 random replications by the state-of-the-art K-means++ scheme [1] speaks volume for the merit of the proposed semi-convex relaxation scheme used by KindAP. Since the running time of KindAP+L is at the same order of that of a single run of the Matlab kmeans function, in essence KindAP+L is thousands of times faster than K-means in reaching high accuracies on large-K problems.

In the previous section, we claim that the iteration complexity of KindAP is linear with respect to the size of datasets, but the efficiency of KindAP also depends on the number of iterations required for convergence. In practice, we observe that KindAP only takes several outer iterations and dozens of inner iterations on the 35 datasets (see more details in the supplementary material).

### 6.3 Datasets with deep neural network features

Deep neural network (DNN) is the trend of data mining. Recently, many deep clustering techniques have been developed to achieve higher clustering accuracy on big datasets. In this section, we select 5 image datasets, ORL, CIFAR100 (train and test), COIL100 and UKBench and process them using a

DNN procedure as follows. We input the raw data into a pre-trained neural network [13], then extract features represented by neurons at a fully-connected layer (usually second from the last). Afterwards, we do ordinary spectral embeddings and apply KM, SR and KindAP on these DNN features.

To be specific, we extract features from Layer avg pool of DNN Xception to cluster ORL, COIL100 and UKBench, and from Layer fc2 of DNN VGG-16 to cluster CIFAR100, see [13], with weights pre-trained on ImageNet. All network architecture and pre-trained weights are provided by the Python Deep Learning library Keras. Since data augmentation techniques and batch sizes do not make much differences to the final results, we select the default settings. Lastly, we do 30 random replications for K-means and SR.

Datasets	$k$	KindAP	SR 30	KindAP+L	KM 30
ORL	40	86.50%/ <b>0.04</b>	86.50%/0.21	86.25%/0.05	86.25%/0.57
CIFAR100(train)	100	<b>99.63%/3.75</b>	84.80%/16.51	99.62%/6.53	94.40%/113.22
CIFAR100(test)	100	<b>68.98%/0.72</b>	67.85%/4.45	65.48%/1.59	61.54%/ 52.23
COIL100	100	<b>98.71%/1.15</b>	81.14%/ 3.61	98.70%/1.53	97.67%/ 16.58
UKBench	2550	89.67%/ <b>4034</b>	82.40%/ 4727	<b>89.93%/4602</b>	84.62%/17270

Table 2: Clustering accuracy and timing based on pre-trained DNN features

Table 2 summarizes the performance of the four algorithms on clustering the DNN features. It shows that KindAP and KindAP+L are generally more accurate than SR and K-means with 30 random replications. We reiterate that our study is not about preprocessing techniques but about clustering methodologies. However, the use of DNN techniques that produce clustering-friendly features does enable us to better evaluate the performance of different clustering methods. On poorly processed data, one would hardly be able to differentiate behaviors of methods because all of them would produce almost equally poor clustering results.

In terms of timing, KindAP is usually slower than the average running time per replication of either Lloyd or SR, but at the same order. However, both Lloyd and SR require multiple replications in order to have a chance to reach an accuracy level comparable with that of KindAP (sometimes they could only reached a lower level of accuracy after a huge number of replications). As is indicated by the results in Table 2, KindAP runs much faster than KM 30 and SR 30 while attaining higher accuracies. In fact, the current version of the KindAP algorithm is still far from optimal in efficiency, and we are working on new algorithms to accelerate the solution time in solving the semi-convex relaxation model.

To summarize our numerical experiments, we list several observations. (i) KindAP and KindAP+L are essentially deterministic without the need for random replications. (ii) On small-K problems, KindAP+L works as well as the classic K-means with very large numbers of replications. (iii) On large-K problems, KindAP and KindAP+L generally outperform their counterparts SR and Lloyd with multiple replications. (iv) The advantages of KindAP appears more pronounced with high dimensional but clustering-friendly features extracted by advanced DNN techniques.

## 7 Conclusions

Data clustering usually consists of two tasks: first extracting suitable features and then applying a clustering method. The focus of this work is on the latter task for which the method of choice has arguably been K-means. We propose the K-indicators framework (5) that includes the classic K-means model (3) and the particular K-indicators model (9) corresponding to two different subspace distances. We promote the K-indicators model (9) because it has a convex objective function and allows an effective semi-convex-relaxation scheme, leading to the construction of an efficient algorithm called KindAP, which is essentially deterministic without any need for random replications. Like the K-means algorithm, KindAP keeps the per-iteration complexity linear in terms of the sizes of datasets, making it practical for big-volume data clustering.

For synthetic data with separable clusters, experiments show that K-indicators can overcome the big-K bottleneck suffered by K-means (see Fig. 1). Is this advantage really relevant in real-world applications? Our experiment results in Tables 1-2 strongly suggest an affirmative answer. On the one hand, more and more big data applications come with large K values. On the other hand, the

advances in feature extraction techniques, especially those using deep neural networks, make it possible to generate clustering-friendly or even nearly separable clusters in feature spaces. Therefore, a deterministic clustering method like KindAP that is scalable to  $K$  and linear in the dataset size will clearly become more desirable than  $K$ -means that suffers from the big- $K$  bottleneck due to its over-sensitivity to initializations.

We note that the  $K$ -means model (3) and the  $K$ -indicators model (9) are two distinct models that in general produce different clustering results at optimality. However, the two models are close enough (see (8)) so that KindAP results can be used to initialize  $K$ -means. Our experiments show that a single KindAP initialization can generate better clustering results, as measured by the  $K$ -means objective, than those generated from large numbers of replications using the current state-of-the-art initialization. A limitation of KindAP is that it requires, at least in theory, the input data matrices to be orthogonal, which is always the case in spectral clustering or similar settings.

Finally, we mention that the development of a theoretic foundation for the KindAP algorithm is an on-going effort that will be reported in a future work.

### Acknowledgments

Y. Yang and Y. Zhang would like to acknowledge the support from NFS Grant DMS-1418724 and from the Shenzhen Research Institute of Big Data (SRIBD). The work of L. Xu is partially supported by a Key Project of the Major Research Plan of NSFC (Grant No. 91630205)

### References

- [1] David Arthur and Sergei Vassilvitskii.  $k$ -means++: The advantages of careful seeding. In *Proceedings of the eighteenth annual ACM-SIAM symposium on Discrete algorithms*, pages 1027–1035. Society for Industrial and Applied Mathematics, 2007.
- [2] Pranjal Awasthi, Afonso S Bandeira, Moses Charikar, Ravishankar Krishnaswamy, Soledad Villar, and Rachel Ward. Relax, no need to round: Integrality of clustering formulations. In *Proceedings of the 2015 Conference on Innovations in Theoretical Computer Science*, pages 191–200. ACM, 2015.
- [3] Ake Björck and Gene H Golub. Numerical methods for computing angles between linear subspaces. *Mathematics of Computation*, 27(123):579–594, 1971.
- [4] Christos Boutsidis, Petros Drineas, and Michael W Mahoney. Unsupervised feature selection for the  $k$ -means clustering problem. In *Advances in Neural Information Processing Systems*, pages 153–161, 2009.
- [5] Deng Cai, Xiaofei He, and Jiawei Han. Document clustering using locality preserving indexing. *IEEE Transactions on Knowledge and Data Engineering*, 17(12):1624–1637, 2005.
- [6] Xi Chen, Yan Duan, Rein Houthoofd, John Schulman, Ilya Sutskever, and Pieter Abbeel. Infogan: Interpretable representation learning by information maximizing generative adversarial nets. In *Advances in neural information processing systems*, pages 2172–2180, 2016.
- [7] Yizong Cheng. Mean shift, mode seeking, and clustering. *IEEE transactions on pattern analysis and machine intelligence*, 17(8):790–799, 1995.
- [8] Eric C Chi and Kenneth Lange. Splitting methods for convex clustering. *Journal of Computational and Graphical Statistics*, 24(4):994–1013, 2015.
- [9] Inderjit S Dhillon, Yuqiang Guan, and Brian Kulis. Kernel  $k$ -means: spectral clustering and normalized cuts. In *Proceedings of the tenth ACM SIGKDD international conference on Knowledge discovery and data mining*, pages 551–556. ACM, 2004.
- [10] Chris Ding and Xiaofeng He.  $K$ -means clustering via principal component analysis. In *Proceedings of the twenty-first international conference on Machine learning*, page 29. ACM, 2004.
- [11] Chris HQ Ding, Tao Li, and Michael I Jordan. Convex and semi-nonnegative matrix factorizations. *IEEE transactions on pattern analysis and machine intelligence*, 32(1):45–55, 2010.
- [12] Brendan J Frey and Delbert Dueck. Clustering by passing messages between data points. *science*, 315(5814):972–976, 2007.

- [13] Joris Guerin and Byron Boots. Improving image clustering with multiple pretrained cnn feature extractors. *british machine vision conference*, page 51, 2018.
- [14] Toby Dylan Hocking, Jeanphilippe Vert, Armand Joulin, and Francis R Bach. Clusterpath: an algorithm for clustering using convex fusion penalties. pages 745–752, 2011.
- [15] Jin Huang, Feiping Nie, and Heng Huang. Spectral rotation versus k-means in spectral clustering. pages 431–437, 2013.
- [16] Pan Ji, Tong Zhang, Hongdong Li, Mathieu Salzmann, and Ian Reid. Deep subspace clustering networks. In *Advances in Neural Information Processing Systems*, pages 24–33, 2017.
- [17] Fredrik Lindsten, Henrik Ohlsson, and Lennart Ljung. Just relax and come clustering!: A convexification of k-means clustering. 2011.
- [18] Stuart P Lloyd. Least squares quantization in pcm. *IEEE Transactions on Information Theory*, 28(2):129–137, 1982.
- [19] James MacQueen et al. Some methods for classification and analysis of multivariate observations. In *Proceedings of the fifth Berkeley symposium on mathematical statistics and probability*, volume 1, pages 281–297. Oakland, CA, USA., 1967.
- [20] Andrew Y Ng, Michael I Jordan, and Yair Weiss. On spectral clustering: Analysis and an algorithm. In *Advances in neural information processing systems*, pages 849–856, 2002.
- [21] Online. ORL dataset. <http://www.cl.cam.ac.uk/research/dtg/attarchive/facedatabase.html>.
- [22] Jiming Peng and Yu Wei. Approximating k-means-type clustering via semidefinite programming. *SIAM Journal on Optimization*, 18(1):186–205, 2007.
- [23] Xi Peng, Shijie Xiao, Jiashi Feng, Wei-Yun Yau, and Zhang Yi. Deep subspace clustering with sparsity prior. In *IJCAI*, pages 1925–1931, 2016.
- [24] Alex Rodriguez and Alessandro Laio. Clustering by fast search and find of density peaks. *Science*, 344(6191):1492–1496, 2014.
- [25] Bernhard Schölkopf, Alexander Smola, and Klaus-Robert Müller. Nonlinear component analysis as a kernel eigenvalue problem. *Neural computation*, 10(5):1299–1319, 1998.
- [26] Sohil Shah and Vladlen Koltun. Robust continuous clustering. *Proceedings of the National Academy of Sciences of the United States of America*, 114(37):9814–9819, 2017.
- [27] Uri Shaham, Kelly P Stanton, Henry Li, Ronen Basri, Boaz Nadler, and Yuval Kluger. Spectralnet: Spectral clustering using deep neural networks. *international conference on learning representations*, 2018.
- [28] Jianbo Shi and Jitendra Malik. Normalized cuts and image segmentation. *IEEE Transactions on pattern analysis and machine intelligence*, 22(8):888–905, 2000.
- [29] Robin Sibson. Slink: an optimally efficient algorithm for the single-link cluster method. *The computer journal*, 16(1):30–34, 1973.
- [30] J von Neumann. Functional operators. vol. ii. the geometry of orthogonal spaces, volume 22 (reprint of 1933 notes) of annals of math. *Studies. Princeton University Press*, 1950.
- [31] Wei Xu, Xin Liu, and Yihong Gong. Document clustering based on non-negative matrix factorization. In *Proceedings of the 26th annual international ACM SIGIR conference on Research and development in informaion retrieval*, pages 267–273. ACM, 2003.
- [32] Yu and Shi. Multiclass spectral clustering. pages 313–319, 2003.
- [33] Hongyuan Zha, Xiaofeng He, Chris H Q Ding, Ming Gu, and Horst D Simon. Spectral relaxation for k-means clustering. pages 1057–1064, 2001.
- [34] Tian Zhang, Raghu Ramakrishnan, and Miron Livny. Birch: an efficient data clustering method for very large databases. In *ACM Sigmod Record*, volume 25, pages 103–114. ACM, 1996.

## 8 Supplementary Material

### 8.1 Proof of Theorem 3.1

*Proof.* It is easy to verify that  $\text{dist}(\mathcal{R}(\hat{U}), \mathcal{R}(H)) := \min_{R^T R=I} \{\|\hat{U}R - H\|_F : R \in \mathbb{R}^{k \times k}\}$  satisfies the non-negativity, identity of indiscernibles and symmetricity, and it suffices to show  $\text{dist}$  satisfies triangle inequality.

First, let  $V^i \in \mathbb{R}^{n \times k}$  for  $i = 1, \dots, 3$  are three orthonormal matrices, and denote  $R^{ij}$  as the optimal solutions of the following optimization problems:

$$R^{ij} = \operatorname{argmin}_{R^T R=I} \|V^i R - V^j\|_F \quad \text{for } 1 \leq i, j \leq 3, \quad \text{and } i \neq j.$$

Then, we have

$$\begin{aligned} \text{dist}(\mathcal{R}(V^1), \mathcal{R}(V^3)) &= \|V^1 R^{13} - V^3\|_F \\ &\leq \|V^1 R^{12} R^{23} - V^3\|_F \\ &= \|V^1 R^{12} R^{23} - V^2 R^{23} + V^2 R^{23} - V^3\|_F \\ &\leq \|V^1 R^{12} - V^2\|_F + \|V^2 R^{23} - V^3\|_F \\ &= \text{dist}(\mathcal{R}(V^1), \mathcal{R}(V^2)) + \text{dist}(\mathcal{R}(V^2), \mathcal{R}(V^3)) \end{aligned}$$

Therefore, the function  $\text{dist}(\mathcal{R}(\hat{U}), \mathcal{R}(H)) := \min_{R^T R=I} \{\|\hat{U}R - H\|_F : R \in \mathbb{R}^{k \times k}\}$  defines a distance between  $\mathcal{R}(\hat{U})$  and  $\mathcal{R}(H)$ .

For fixed  $H \in \mathcal{H}$ , the closed form solution of the optimization problem  $\min_{R^T R=I} \|\hat{U}R - H\|_F$  is given by  $R^* = PQ^T$ , where  $\hat{U}^T H = P\Sigma Q^T$  is a singular value decomposition of  $\hat{U}^T H$ , and its optimum value is given by

$$\begin{aligned} \min_{R^T R=I} \|\hat{U}R - H\|_F^2 &= \|\hat{U}R^*\|_F^2 + \|H\|_F^2 - 2\text{Tr}(R^{*T} \hat{U}^T H) \\ &= 2k - 2\text{Tr}[(PQ^T)^T P\Sigma Q^T] \\ &= 2k - 2\text{Tr}(\Sigma) \\ &= 2k - 2\|\hat{U}^T H\|_* \\ &= 2k - 2 \sum_{j=1}^k \sigma_j(\hat{U}^T H) \end{aligned}$$

Therefore,

$$\min_{H \in \mathcal{H}} \text{dist}^2(\mathcal{R}(\hat{U}), \mathcal{R}(H)) = \min_{H \in \mathcal{H}} \min_{R^T R=I} \|\hat{U}R - H\|_F^2 \quad (16)$$

$$\Leftrightarrow \max_{H \in \mathcal{H}} \|\hat{U}^T H\|_* \Leftrightarrow \max_{H \in \mathcal{H}} \sum_{j=1}^k \sigma_j(\hat{U}^T H). \quad (17)$$

Moreover,

$$\begin{aligned} \frac{1}{2} \|\hat{U}\hat{U}^T - HH^T\|_F^2 &= k - \|\hat{U}^T H\|_F^2 \\ &= k - 2\text{Tr}(\hat{U}^T H) + k \\ &\quad - (k - 2\text{Tr}(\hat{U}^T H) + \|\hat{U}^T H\|_F^2) \\ &= \|\hat{U} - H\|_F^2 - \|I - \hat{U}^T H\|_F^2 \\ &\leq \|\hat{U} - H\|_F^2 \end{aligned}$$

Note that the above inequality always holds when we replace  $\hat{U}$  by  $\hat{U}R$  for any orthogonal  $R$ , therefore

$$\frac{1}{2} \|\hat{U}\hat{U}^T - HH^T\|_F^2 \leq \min_{R^T R=I} \|\hat{U}R - H\|_F^2 \quad (18)$$

The singular values of  $\hat{U}^T H$  are the cosines of the principle angles between  $\mathcal{R}(\hat{U})$  and  $\mathcal{R}(H)$ , so  $0 \leq \sigma_j \leq 1$ , which implies  $\sigma_j^2 \leq \sigma_j$ . This claim can also be derived through  $\sigma_j \leq \|\hat{U}^T H\|_2 \leq \|\hat{U}\|_2 \|H\|_2 = 1$ . Therefore, we prove the right part of inequality (8).

$$\frac{\sqrt{2}}{2} \|\hat{U}\hat{U}^T - HH^T\|_F \leq \min_{R^T R=I} \|\hat{U}R - H\|_F \leq \|\hat{U}\hat{U}^T - HH^T\|_F \quad (19)$$

□

## 8.2 Identical performance on 29 small-K datasets

Table 3 gives the characteristics of the 35 datasets used in the paper. Table 4 compares the performance of KindAP+L and KM 10000 on 29 “small-K” ( $k \leq 20$ ) datasets.

Dataset	No. of Clusters	No. of Samples	No. of Attributes
Australian	2	690	14
Breast	2	699	10
Chess	2	3196	36
Crx	2	690	15
Diabetes	2	768	8
Heart	2	270	13
Isolet	2	1560	617
Monk1	2	432	6
Pima	2	768	8
Vote	2	435	16
Cars	3	392	8
Iris	3	150	4
Lenses	3	24	4
Waveform-21	3	2746	21
WINE	3	178	13
Auto	6	205	25
Control	6	600	60
Dermatology	6	366	34
glass	6	214	9
Solar	6	323	12
Segment	7	2310	19
ZOO	7	101	16
Ecoli	8	336	343
Yeast	10	1484	1470
JAFFE	10	180	4096
USPS	10	9298	256
MNIST6000	10	6000	784
YALE	15	165	4096
COIL20	20	1440	1024
YALEB	38	2414	1024
ORL	40	400	4096
Reuters	65	8293	18933
PIE	68	11554	1024
FERET	72	432	10304
AR	120	1680	2000

Table 3: The characteristics of 35 Datasets

Datasets	$k$	Clustering Accuracy		Objective Value	
		KindAP+L	KM 10000	KindAP+L	KM 10000
Australian	2	68.70%	68.70%	1.530017e-01	1.530017e-01
Breast	2	51.94%	51.94%	2.413292e-02	2.413292e-02
Crx	2	53.33%	53.33%	1.304456e-01	1.304456e-01
Diabetes	2	64.71%	64.71%	6.455858e-02	6.455858e-02
Heart	2	62.22%	62.22%	3.106905e-01	3.106905e-01
Isolet	2	59.29%	59.29%	1.568688e-01	1.568688e-01
Monk1	2	66.90%	66.90%	1.568688e-01	1.568688e-01
Pima	2	65.36%	65.36%	3.827793e-01	3.827793e-01
Vote	2	56.78%	56.78%	1.318960e-01	1.318960e-01
Cars	3	67.60%	67.60%	2.180936e-01	2.180936e-01
Iris	3	67.60%	67.60%	2.244802e-01	2.244802e-01
Lenses	3	41.67%	41.67%	6.056203e-01	6.056203e-01
Waveform-21	3	52.37%	52.37%	3.746717e-01	3.746717e-01
WINE	3	61.80%	61.80%	3.761429e-01	3.761429e-01
Auto	6	32.68%	32.68%	5.431086e-01	5.431086e-01
Control	6	58.33%	58.33%	4.644075e-01	4.644075e-01
Dermatology	6	95.90%	95.90%	3.648208e-01	3.648208e-01
glass	6	50.47%	50.47%	1.135033e+00	1.135033e+00
Solar	6	37.15%	37.15%	5.693965e-01	5.693965e-01
Segment	7	41.43%	41.43%	5.369213e-01	5.369213e-01
ZOO	7	51.49%	51.49%	4.726120e-01	4.726120e-01
Ecoli	8	56.55%	56.55%	2.058497e+00	2.058497e+00
Yeast	10	31.74%	31.74%	8.848088e-02	8.848088e-02
JAFFE	10	62.22%	62.22%	1.351849e+00	1.351849e+00
USPS	10	66.78%	66.78%	1.394255e+00	1.394255e+00
MNIST6000	10	63.38%	63.38%	1.777071e+00	1.777071e+00
YALE	15	56.36%	56.36%	1.855949e+00	1.855949e+00
COIL20	20	82.01%	82.01%	1.365658e+00	1.365658e+00

Table 4: Identical clustering performance of two algorithms on 29 small-K datasets.

Table 5 demonstrates the convergence behaviors of KindAP on the 35 datasets. For each outer iteration (from  $\mathcal{U}$  to  $\mathcal{H}$  and back to  $\mathcal{U}$ ), we record the number of inner iterations required for convergence (alternating projections between  $\mathcal{U}$  and  $\mathcal{N}$ ), and the total numbers of outer and inner iterations (in parentheses) are reported in the last column.

We observe that in KindAP the first outer iteration takes the most number of inner iterations. In fact, the first outer iteration also makes the most significant progress. In particular, on the datasets Breast and Chess KindAP converges after only one outer iteration in which the K-indicators objective arrives at the global optimal value zero (subject to round-off error).

We also did another experiment in which after each KindAP outer iteration, we calculate cluster centers from the current solution and start the Lloyd algorithm to solve the K-means model. Interestingly, on all the 29 datasets in Table 4 the Lloyd algorithm returns identical K-means results after the first KindAP outer iteration. That is, for solving the K-means model, only one KindAP outer iteration is necessary to generate a set of centers that allows the Lloyd algorithm to produce the presumably global optimum without any further replication. On the other hand, after the first outer iteration until it stops, KindAP continues to improve the K-indicators objective value. This again highlights the fact that these two models are distinct.

Outer Iterations	1	2	3	4	5	6	7	Total
Australian	9	4	—	—	—	—	—	2(13)
Breast	24	—	—	—	—	—	—	1(24)
Chess	23	—	—	—	—	—	—	1(23)
Crx	17	3	—	—	—	—	—	2(20)
Diabetes	12	3	—	—	—	—	—	2(15)
Heart	8	2	—	—	—	—	—	2(10)
Isolet	8	2	—	—	—	—	—	2(10)
Monk1	8	2	—	—	—	—	—	2(10)
Pima	12	4	—	—	—	—	—	2(16)
Vote	9	4	—	—	—	—	—	2(13)
Cars	8	2	—	—	—	—	—	2(10)
Iris	11	2	—	—	—	—	—	2(13)
Lenses	40	4	—	—	—	—	—	2(44)
Waveform-21	9	3	3	—	—	—	—	2(15)
WINE	15	3	—	—	—	—	—	2(18)
Auto	14	4	—	—	—	—	—	2(18)
Control	13	4	—	—	—	—	—	2(17)
Dermatology	12	4	—	—	—	—	—	2(16)
glass	34	5	—	—	—	—	—	2(39)
Solar	9	4	—	—	—	—	—	2(13)
Segment	12	5	—	—	—	—	—	2(17)
ZOO	12	4	—	—	—	—	—	2(16)
Ecoli	12	4	—	—	—	—	—	2(16)
Yeast	15	4	—	—	—	—	—	2(19)
JAFFE	14	4	—	—	—	—	—	2(18)
USPS	14	4	4	4	—	—	—	2(15)
MNIST6000	20	4	4	4	—	—	—	4(32)
YALE	25	4	—	—	—	—	—	2(29)
COIL20	14	4	—	—	—	—	—	2(18)
YALEB	26	4	5	5	—	—	—	4(40)
ORL	50	6	5	4	4	—	—	5(69)
Reuters	37	4	4	4	4	4	—	6(57)
PIE	35	5	5	5	—	—	—	4(50)
FERET	48	5	5	5	5	5	—	6(73)
AR	41	5	5	5	5	—	—	5(61)

Table 5: The convergence behavior of KindAP on 35 Datasets

### 8.3 Uncertainty information

In unsupervised learning, it is usually difficult to evaluate the performance due to the absence of ground truth. People mostly use clustering accuracy and normalized mutual information, but both require ground truth. However, the proposed KindAP algorithm is able to provide some *a posteriori* information as a metrics of performance. An output of KindAP algorithm is a non-negative matrix  $N$ , which generally contains more than one positive elements on each row. It is observed in practice that the magnitude of  $[N]_{ij} \geq 0$  is positively proportional to the probability that data point  $i$  is in cluster  $j$ . Let  $\hat{N}$  hold the elements of  $N$  sorted row-wise in a descending order, we define a *soft indicator vector*  $s$ , which takes values between zero and one as follows,

$$s_i = 1 - [\hat{N}]_{i2}/[\hat{N}]_{i1} \in [0, 1], \quad i = 1, \dots, n, \quad (20)$$

where the ratio is between the second largest and the largest elements on the  $i$ -th row of  $N$ . It is intuitive to expect that the closer to zero  $s_i$  is, the more uncertain about the assignment to this data object, which means it is more probable that the data object  $i$  belongs to more than one cluster. In

contrast,  $s_i$  close to one implies a safe clustering assignment. This intuition is clearly validated in the simple example presented in Fig. 4A. The results in Fig. 4B show the relationship between the soft indicator and clustering accuracy on a face image dataset, ORL. We observe that large soft indicator values on average indicate high KindAP clustering accuracy. This soft indicator offered by the KindAP algorithm helps address the very challenging issue of assessing the quality and uncertainty of clustering assignments in the absence of ground truth.

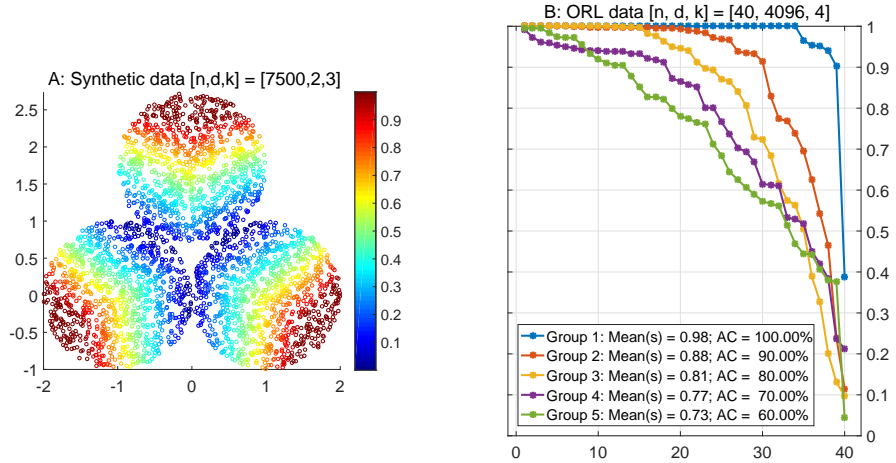


Figure 4: Soft indicators. In plot (A), the dataset consists of three circular clusters in  $\mathbb{R}^2$ , mutually tangential to each other. Then 2500 points are uniformly placed inside each circle. Plot (A) shows the distribution of the points colored according to their KindAP-generated soft indicator values, which clearly are highly correlated to the distance to neighboring clusters. Plot (B) was generated as follows. Five groups were selected from ORL dataset [21], each containing 40 face images taken from 4 individuals with a varying degree of similarity. For each group, KindAP was applied to the first 4 leading eigenvectors of the normalized Laplacian of a similarity graph, where the similarity graph is built according to [5]. Plot (B) gives the resulting 5 soft indicators sorted in an ascending order. Corresponding clustering accuracy and the mean of the soft indicator are also recorded for the 5 groups, showing a clear correlation between the two quantities.